Chemical Engineering Journal 99 (2004) 131–136

Chemical Engineering Journal

www.elsevier.com/locate/cej

Kinetic study of *iso*-octane steam reforming over a nickel-based catalyst

Praharso, A.A. Adesina [a], D.L. Trimm*, N.W. Cant [b]

[a] *School of Chemical Engineering and Industrial Chemistry, The University of New South Wales, Sydney 2052, Australia*
[b] *Department of Chemistry, Macquarie University, Sydney 2109, Australia*

Received 9 March 2003; accepted 4 October 2003

Abstract

The kinetics of *iso*-octane steam reforming over a nickel based catalyst has been examined as a function of *iso*-octane and steam partial pressures at various temperatures. The reaction order is 0.2 with respect to *iso*-octane, suggesting strong coverage of nickel by *iso*-octane and 0.5 with respect to steam, indicating dissociative adsorption of steam. Indeed, a Langmuir–Hinshelwood (LH) mechanism requiring the dissociative adsorption of *iso*-octane and steam on two different sites appeared to be the most plausible pathway for the steam reforming reaction. The activation energy of $44 \pm 2.2\,\mathrm{kJ\,mol^{-1}}$ estimated from the LH model is consistent with the trend previously reported for other lower hydrocarbons.

Keywords: Gasoline; *iso*-Octane; Kinetic; Nickel; Steam reforming

1. Introduction

The control of vehicle exhaust emissions using catalytic converters has been highly successful [1]. However, increasingly stringent legislation demands emission control that is at or beyond the capability of conventional catalysts and alternative means of reducing emissions are under consideration. Of these, fuel cell powered vehicles based on the polymer electrolyte membrane fuel cell (PEMFC) are favoured but these cells have the disadvantage of operating only on hydrogen as a fuel [2]. Since the distribution and on-board storage of hydrogen presents very real problems, attention has been focused on the conversion of more readily available fuels to hydrogen on board the vehicle. The partial oxidation of hydrocarbons is one approach [3], namely,

$$CH_4 + \tfrac{1}{2}O_2 \leftrightarrow CO + 2H_2, \quad \Delta H_{298} = -36\,\mathrm{kJ\,mol^{-1}}$$

Alternatively, conversion may be effected via steam or CO_2 reforming [3]

$$CH_4 + H_2O \leftrightarrow CO + 3H_2, \quad \Delta H_{298} = 206.2\,\mathrm{kJ\,mol^{-1}}$$

$$CH_4 + CO_2 \leftrightarrow CO_2 + 2H_2, \quad \Delta H_{298} = 247\,\mathrm{kJ\,mol^{-1}}$$

All reactions are favoured at high temperatures and require initiation, usually achieved by combusting part of the fuel [3]

$$CH_4 + 2O_2 \leftrightarrow CO_2 + 2H_2O, \quad \Delta H_{298} = -802\,\mathrm{kJ\,mol^{-1}}$$

Exothermic partial oxidation is self-sustaining, once initiated, while endothermic reforming reactions require continuing heat supplied by combustion (autothermal reforming [2]).

The production of hydrogen from methane [4], methanol [5] and light hydrocarbons [4] has been reported. The present studies are focused on the conversion of *iso*-octane used as a model for gasoline

$$C_8H_{18} + \tfrac{25}{2}O_2 \leftrightarrow 8CO_2 + 9H_2O, \quad \Delta H_{298} = -5100.6\,\mathrm{kJ\,mol^{-1}} \tag{1}$$

$$C_8H_{18} + 4O_2 \leftrightarrow 8CO + 9H_2, \quad \Delta H_{298} = -659.9\,\mathrm{kJ\,mol^{-1}} \tag{2}$$

$$C_8H_{18} + 8H_2O \leftrightarrow 8CO + 17H_2, \quad \Delta H_{298} = 1274.8\,\mathrm{kJ\,mol^{-1}} \tag{3}$$

$$CO + H_2O \leftrightarrow CO_2 + H_2, \quad \Delta H_{298} = -41.2\,\mathrm{kJ\,mol^{-1}} \tag{4}$$

* Corresponding author. Tel.: +61-2-9385-4340; fax: +61-2-9385-5966.
E-mail address: d.trimm@unsw.edu.au (D.L. Trimm).

1385-8947/$ – see front matter © 2003 Elsevier B.V. All rights reserved.
doi:10.1016/j.cej.2003.10.002

Studies of the partial oxidation of *iso*-octane (reaction (2)) have been reported elsewhere [6] as have studies of the complete combustion of the fuel [7]. It was found that the optimal arrangement for the heavier fuel involved heat generation by total oxidation on a supported Pt-based catalyst, followed by steam reforming over a Ni-based catalyst [8]. The present paper reports the kinetics of the steam reforming reaction and relates these to the overall oxidation/reforming system.

2. Experimental

Typically, about 0.3 g of a commercial steam reforming alumina-supported Ni catalyst was diluted with α-$A1_2O_3$ particles in the weight ratio 1:9. Although for proprietary reasons, the actual composition of the catalyst is not provided, it was prepared by co-precipitation of the appropriate metal nitrates, followed by calcination at a temperature greater than 1273 K [9] before delivery to our laboratory. Before use, the catalyst was further treated in situ in a flow of 100 ml min^{-1} of 20% H_2/N_2 at 873 K for 4 h.

iso-Octane was vaporised from two saturators at 293 K using nitrogen as the carrier gas. Water at various flow rates was supplied by an ISCO 260D syringe pump. All reactants passed through a preheater at 473 K. A stainless steel fixed bed reactor (i.d.=10 mm) was used for all experiments. Gas flows were metered and regulated by Brooks mass flow controllers (Model 5850 E). Products, CO_2, CO, H_2, CH_4, unreacted *iso*-octane and occasionally small amounts of acetylene, were analysed by gas chromatography (FID-GC for *iso*-octane and TCD-GC for the lighter products). Rate measurements were subsequently obtained from differential analysis of the concentration–time data. *iso*-Octane conversion was maintained at 10–20% for all temperatures investigated. The absence of pore diffusion was confirmed with tests using catalyst with three different particle sizes between 200 and 500 μm. Rate was practically invariant over this particle size range. However, in order to avoid high reactor bed pressure drop (<5 kPa), kinetic runs were conducted with the particle fraction in the 300–425 μm bracket. Initial experiments also indicated that reaction rate was unchanged at total gas flow rate above 300 ml min^{-1}, suggesting the absence of external transport resistance and hence, the choice of 60,000 ml g cat^{-1} h^{-1} as the operating space velocity. Preliminary stability tests were done at 623 K and a steam–carbon (S:C) ratio of three for 24 h with no sign of carbon formation. Carbon balances were maintained for each run within ±5%.

The orders of reaction with respect to *iso*-octane and steam were determined by following the rate of *iso*-octane consumption under various combinations of *iso*-octane and steam partial pressures but ensuring that the steam–carbon ratio was at a minimum of 3 to avoid carbon deposition and a maximum of 7 to avoid re-oxidation of reduced Ni. This corresponded to a partial pressure of steam between 6.15 and 56.92 kPa. The partial pressure of *iso*-octane was varied between 0.28 and 1.47 kPa. Rate measurements were made at 583, 603 and 623 K at a constant space velocity.

The catalyst was thermally characterised by temperature-programmed reduction (TPR) with the aid of a Micromeritics Autochem 2910. Nickel metallic surface area was investigated on the same unit using hydrogen pulse-chemisorption at 323 K. The multi-point BET surface area was measured by a Micromeritics Tristar 3000 under liquid nitrogen temperature and using nitrogen as an adsorbate.

3. Results and discussions

3.1. Fresh catalyst characterisation results

The BET surface area of Ni catalyst was 11 ± 0.2 m^{-2} $g^{-1}$with an average pore size of 21.2 nm. This relatively low surface area for an alumina-supported catalyst is in agreement with the high temperature calcination ($T > 1273$ K) employed in the catalyst preparation and indicate that the alumina support was probably in the α-phase. Fig. 1 shows a TPR profile for Ni catalyst. The sample was pretreated by helium at 383 K and then cooled to ambient temperature. A 5% H_2/N_2 was used as a reducing medium and the temperature was ramped at 2 K min^{-1} from ambient to 873 K. A bulk reduction temperature located at 620 K is comparable to the value of 573 K previously reported by Ma [4]. The shift in peak may be due to the different heating rate employed. Since the catalyst was supplied as a high temperature calcined solid, it is unlikely that the shoulder peaks at 543 and 668 K are due to loss of promoters. However, they may be attributed to the reduction of low temperature metal aluminates. The absence of other peaks up to 873 K showed that metal active sites for the *iso*-octane steam reforming belonged to reducible metal oxides below this temperature. Ma [4] had found that NiO was, however, completely reduced at 673 K.

H_2 chemisorption measurements at 323 K gave a metal surface area of 0.51 m^{-2} g cat^{-1} with a corresponding metal particle size of 337 nm and a low metal dispersion of 0.3%. These estimates are consistent with the high metal loading on the support. Corresponding estimates using CO adsorption (assuming nondissociative CO adsorption of one molecule per Ni site) given in Table 1 also confirmed that Ni metal surface area and dispersion are relatively low for the catalyst used.

Table 1
Nickel surface area

Chemisorption results	CO [4]	H_2
Ni surface area (m^2 g cat^{-1})	1.78	0.51
Metal dispersion (%)	1.01	0.30
Active particle diameter (nm)	Not available	337

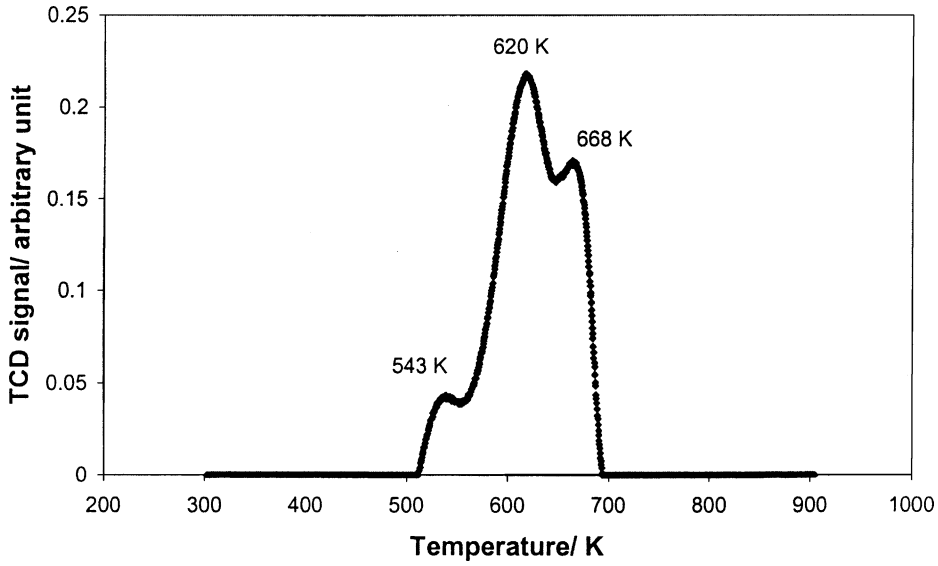

Fig. 1. H_2-TPR profile for nickel catalyst (0.4 g of catalyst, 10 ml min^{-1} reductant, 2 K min^{-1}).

3.2. Modeling of the kinetic data

Kinetic data were collected over the range of reactant partial pressures earlier specified using a Fibonacci search [10]. This strategy is especially advantageous when dealing with inherently nonlinear systems and to minimise 'memory effect' on the response variable. Essentially, the method requires that given a starting point for the independent variable and n number of experiments, the choice of the step length, L_i, from a preceding experiment is effected in such a way as to ensure that the optimum value is traversed and located within the n experiments. This step length is typically the reciprocal of the ith fibonacci number. Obviously, the precision with which the optimum is found increases with n. Details are given in Ref. [10].

Table 2 shows the rate–temperature composition measurements made in this study. A regression of the rate data at all temperatures to the power-law model

$$-r_{SR} = k_0\, e^{-E/RT} p_{iso}^{a} p_{steam}^{b} \quad (5)$$

gave the parameter estimates provided in Table 3. Fig. 2 shows the parity plot.

The activation energy (44 kJ mol^{-1}) obtained for *iso*-octane is consistent with the trend for other (lower) hydrocarbons as reported by Ma [4], Figueiredo [11], Tottrup [12] and Rostrup-Nielsen [13]. A plot of these activation energies as a function of carbon number is given on Fig. 3 for the Ni-based catalysts. Rostrup-Nielsen [13] has also found that for higher hydrocarbons, such as butane, the reaction order approaches zero.

3.3. Mechanistic models

The relatively low reaction order with respect to *iso*-octane partial pressure (power-law fit) is symptomatic of strong adsorption. By the same token, improved activity with high S:C ratio could be due to gas phase (steam) attack of surface carbon or possible chemisoiption of H_2O on sites different from those containing carbon adspecies, followed

Table 2
Rate–composition–temperature data for the runs

Temperature (K)	*iso*-Octane partial pressure (kPa)	Steam partial pressure (kPa)	Rate ($\times 10^7$ mol g cat^{-1} s^{-1})
583	1.12	23.81	12.80
583	1.15	31.16	15.72
583	1.16	39.56	17.22
583	1.15	49.71	19.98
583	1.01	56.92	21.09
583	0.28	6.15	5.55
583	0.57	12.31	6.87
583	1.18	23.99	9.81
583	0.86	17.78	10.81
583	1.47	29.83	12.20
603	1.17	23.79	18.76
603	1.18	32.02	21.64
603	1.19	40.45	24.30
603	1.21	50.21	28.88
603	1.14	56.31	33.44
603	1.51	29.31	23.62
603	0.27	6.07	9.98
603	0.53	12.04	12.22
603	0.93	17.52	19.81
623	1.23	23.77	34.55
623	1.30	31.97	41.22
623	1.30	39.94	43.89
623	1.35	50.18	46.25
623	1.27	53.86	53.32
623	1.54	29.84	39.64
623	0.96	17.76	38.15
623	0.30	6.14	15.60
623	0.57	12.04	19.98

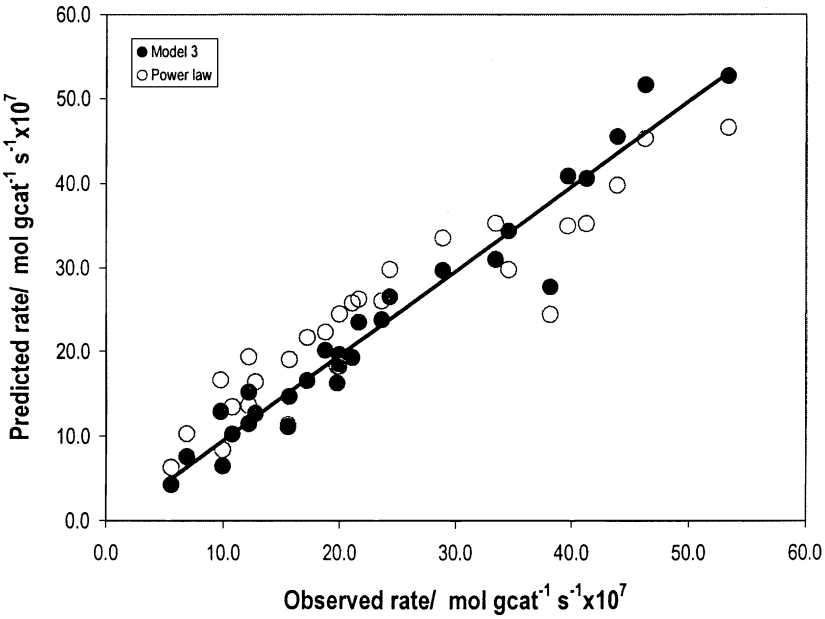

Fig. 2. Predicted (Langmuir–Hinshelwood Model 3 and Power law) vs. observed rate for *iso*-octane steam reforming.

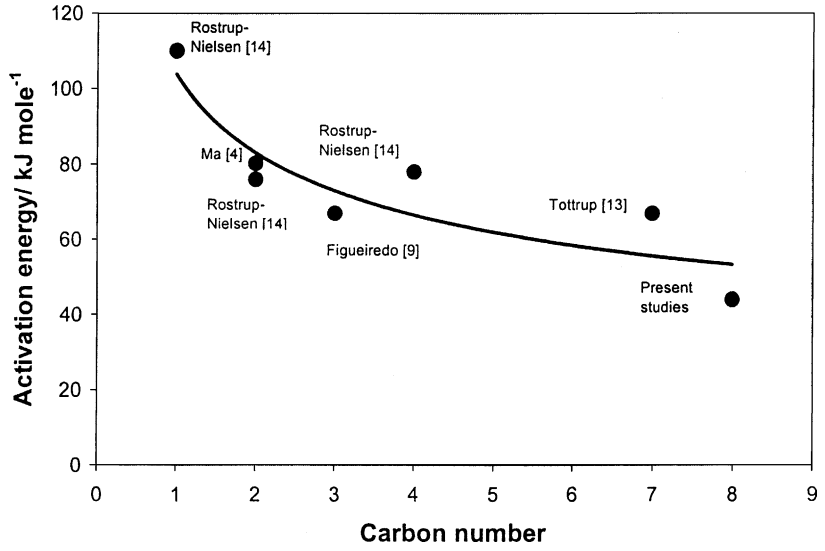

Fig. 3. Activation energies of various hydrocarbons.

by surface reaction. As a result of these considerations, rational Langmuir–Hinshelwood (LH) and Eley–Rideal (ER) models were developed. These models and relevant key features are provided on Table 4.

Table 3
Estimate of parameters for *iso*-octane steam reforming (nonlinear least squares)

Parameter	Unit	Estimates
k_0	mol g cat^{-1} s^{-1} kPa$^{-0.71}$	0.0026 (±0.0001)
E	kJ mol^{-1}	44.0 (±2.2)
a (*iso*-octane order)		0.17 (±0.01)
b (steam order)		0.54 (±0.03)

Values in parentheses show uncertainty.

As reported in Table 5, Models 1–4 gave positive parameter estimates. The remaining models, based on Eley–Rideal mechanism, all gave negative values for one or more of the coefficients and therefore deemed inadequate. Models 1–4 were then assessed using the Boudart–Mears–Vannice [14] guidelines in order to test their thermodynamic consistency. To do so, it was necessary to estimate the entropy and the enthalpy changes of *iso*-octane steam reforming obtained from

$$\ln K = -\Delta H/(RT) + \Delta S/R \quad (6)$$

The thermodynamic constants are presented in Table 6, while the activation energy is reported in Table 7.

Table 4
Theoretical reaction rate models

No.	Model	Remarks
1	$k_{rxn}p_A p_B/(1+k_A p_A + k_B p_B)^2$	Molecular adsorption of both *iso*-octane (A) and steam (B) on the same site followed by bimolecular surface reaction r.d.s.
2	$k_{rxn}p_A p_B/(1+k_A p_A)(1+k_B p_B)$	Dual-site with associative adsorption of *iso*-octane (A) and steam (B) with bimolecular surface r.d.s.
3	$k_{rxn}\sqrt{p_A p_B}/(1+\sqrt{k_A p_A})(1+\sqrt{k_B p_B})$	Dual-site with dissociative adsorption of *iso*-octane (A) and steam (B) and bimolecular surface r.d.s.
4	$k_{rxn}\sqrt{p_A}p_B/(1+\sqrt{k_A p_A}+k_B p_B)^2$	Single-site with dissociative adsorption of *iso*-octane (A) and molecular adsorption of steam (B) followed by bimolecular surface reaction r.d.s.
5	$k_{rxn}p_A p_B/1+k_A p_A$	Eley–Rideal model with associative adsorption of *iso*-octane (A) with steam (B) in gas phase
6	$k_{rxn}\sqrt{p_A}p_B/1+\sqrt{k_A p_A}$	Eley–Rideal model with dissociative adsorption of *iso*-octane (A) with steam (B) in gas phase

Table 5
Estimate of LH models[a]

Model no.	Temperature (°C)	k_{rxn}	K_A	K_B
1	310	1.143E−06	3.230	0.021
	330	1.988E−06	2.815	0.040
	350	2.901E−06	2.246	0.046
2	310	2.842E−05	0.965	10.473
	330	3.817E−05	0.851	9.285
	350	2.901E−05	0.630	8.65
3	310	1.042E−05	0.983	109.683
	330	1.460E−05	0.876	86.204
	350	1.917E−05	0.769	55.153
4	310	1.311E−04	1997.238	0.219
	330	2.133E−04	1759.448	0.314
	350	3.075E−04	1271.281	0.352
5	310	7.017E−05	−1.751	
	330	−5.369E−07	637.527	
6	310	4.194E−05	−0.188	

[a] A: *iso*-octane; B: steam.

For Models 1–4, the adsorption constants of *iso*-octane (K_A obeyed the van't Hoff relation, but the steam adsorption constant (K_B) for Models 1and 4 did not satisfy this expression, since K_B increased as the reaction temperature increased. This phenomenon is not uncommon as reported by Xu and Froment [15] for the steam reforming of methane. As a result, the K_B estimates for Models 1 and 4 did not meet the BMV guidelines.

All rate constants, however, exhibited the Arrhenius-dependency as can be seen in Table 7. Therefore, only Model 3 satisfied thermodynamic scrutiny. On the basis of this assessment, we believe the steam reforming of hydrocarbons may be described by the dual-site mechanism:

$$C_xH_y + 2S_1 \leftrightarrow C_{x-1}H_{y-m_2} - S_1 + C_{m_1}H_{m_2} - S_1 \quad (7)$$

$$H_2O + 2S_2 \leftrightarrow OH - S_2 + H - S_2 \quad (8)$$

$$C_{m_1}H_{m_2} - S_1 + OH - S_2 \rightarrow C_{m_1}H_{m_2}O - S_1 + H - S_2 \quad (9)$$

$$C_{m_1}H_{m_2}O - S_1 + S_1 \rightarrow CO - S_1 + C_{m_1-1}H_{m_2} - S_1 \quad (10)$$

Table 6
Estimates of Models 1–4 for BMV guidelines

Parameter			Correlation coefficient (r^2)	Guidelines no. 1	Guidelines no. 2
ΔH_A (J mol^{-1})	Model 1	−27357	0.98		
	Model 2	−32050	0.94		
	Model 3	−18480	0.99		
	Model 4	−33927	0.93		
ΔS_A (J mol^{-1} K$^{-1)}$	Model 1	−37.0	0.98	37 > 10	37 < 50.5
	Model 2	−55.0	0.94	55 > 10	55 < 57.1
	Model 3	−31.8	0.99	31.8 > 10	31.8 < 38.1
	Model 4	5.3	0.93	No	−5.3 < 59.7
ΔH_B (J mol^{-1})	Model 1	59064	0.89		
	Model 2	−14910	0.99		
	Model 3	−51712	0.96		
	Model 4	35886	0.93		
ΔS_B (J mol^{-1} K^{-1})	Model 1	69.9	0.89	No	Borderline
	Model 2	−61	0.99	No	6.1 < 33.1
	Model 3	−49.3	0.96	49.3 > 10	49.3 < 84.6
	Model 4	−49.2	0.93	No	−49.2 < −38

A: *iso*-octane; B: steam; guideline no. 1: $\Delta S > 10$; guideline no. 2: $\Delta S < (12.2–0.0014\Delta H)$.

Table 7
Estimate of activation energy for Models 1–4

$1/T$ (K^{-1})	$-\ln k$				E (kJ mol^{-1})				Correlation coefficient (r^2)			
	M1	M2	M3	M4	M1	M2	M3	M4	M1	M2	M3	M4
0.00172	13.68	10.47	11.44	8.94	70.4	44.6	43.5	64.4	0.990	0.999	0.999	0.996
0.00166	13.13	10.17	11.13	8.45								
0.00161	12.75	9.88	10.86	8.09								

$$H - S_2 + H - S_2 \rightarrow H_2 \uparrow + 2S_2 \quad (11)$$

$$CO - S_1 \leftrightarrow CO + S_1 \quad (12)$$

where m_1, m_2, x and y are integers. CO_2 may be produced via the water-gas shift reaction but along with other products, has not been included in the adsorption terms in the denominator of the LH models due to the low partial pressures of the product species occasioned by the small conversions employed. Even so, Fig. 2 shows an excellent agreement between observed and predicted rates for Model 3.

The derived kinetic expression can thus be used to predict fuel consumption rate from a compact autothermal fuel processor. The oxidation of *iso*-octane reaches completion faster than steam reforming, and the effect of total oxidation can be considered as a predetermined degree of conversion [8]. It was observed from studies of *iso*-octane oxidation, that the use of oxygen to carbon ratio of 1:1.5 gave about 30–50% of *iso*-octane feed combusted to carbon dioxide and water [16]. The water produced is not sufficient for the steam reforming of the remaining *iso*-octane. As a result, additional water must be injected in the inlet of the reactor and heated by oxidising more fuel. Since the steam:carbon ratio of 3 in the reaction system is required to minimise coke formation, the amount of remaining unburnt *iso*-octane can be predicted from the oxidation reaction, and the minimum amount of additional water and heating required can be estimated. The feasibility of combined oxidation/steam reforming of *iso*-octane and artificial gasoline will be reported in a separate publication.

The kinetics indicate that reaction becomes unacceptably slow below 523 K. Since the steam reforming is endothermic, the temperature at the end of the steam reforming catalyst bed must be above this value while the inlet temperature, which is generated by oxidation of part of the fuel, will be higher.

4. Conclusions

The kinetics of *iso*-octane steam reforming over a nickel-based catalyst has been studied at atmospheric pressure at different temperatures. A power law rate of the form:

$$-r_{SR} = k_0\, e^{-5293.3T}\, p_{C_8C_{18}}^{0.17}\, p_{H_2O}^{0.54} \quad (13)$$

described the data.

Fitting the experimental data to the Langrnuir–Hinshelwood expression shows that the rate determining step in the steam reforming of *iso*-octane involves the reaction between dissociatively adsorbed species of *iso*-octane and steam. The resulting activation energy is comparable to the steam reforming of other hydrocarbons.

Acknowledgements

The authors acknowledge Mr. John Starling and Mr. Phil McAuley for their technical support. Mr. K. Hardiman and Mr. J. Lee are acknowledged for their assistance in operating Micromeritics Autochem 2910. One of the authors [P] is grateful to AusAid for providing a graduate scholarship.

References

[1] E.S.J. Lox, B.H. Engler, in: G. Ertl, H. Knbzinger, J. Weitkamp (Eds.), Handbook of Heterogeneous Catalysis, Weinheim, Germany, VCH, vol. 4, 1997, p. 1559.
[2] D.L. Trimm, Z.I. Önsan, Catal. Rev. Sci. Eng. 43 (2001) 31.
[3] M.A. Pena, J.P. Gomez, J.L.G. Fierro, App. Catal. A: Gen. 144 (1996) 7.
[4] L. Ma, Ph.D. Thesis, University of New South Wales, 1995.
[5] J.L.G. Fierro, Stud. Surf. Sci. Catal. 130 (2000) 177.
[6] Praharso, A.A. Adesina, D.L. Trimm, N.W. Cant, The Korean J. Chem. Eng. 20 (2003).
[7] Praharso, A.A. Adesina, D.L. Trimm, N.W. Cant, unpublished results.
[8] A.K. Avci, Z.I. Onsan, D.L. Trimm, App. Catal. A: Gen. 216 (2001) 243.
[9] J.R.H. Ross, in: M.W. Roberts, J.M. Thomas (Eds.), Surface and Defect Properties of Solids, IV, 35, Specialist Periodical Reports, The Chemical Society, London, 1975, pp. 34–67.
[10] W.H. Ray, J. Szekely, Process Optimization, Wiley, New York, 1973.
[11] J.L. Figueiredo, Ph.D. Thesis, University of London, London, 1975.
[12] P.B. Tottrup, App. Catal. 4 (1982) 377.
[13] J.R. Rostrup-Nielsen, Catalytic Steam Reforming, Springer-Verlag, Berlin, 1984.
[14] M. Boudart, D.E. Mears, M.A. Vannice, Ind. Chim. Beige 32 (1967) 281.
[15] J. Xu, G.F. Froment, AIChE J. 35 (1989) 88.
[16] Praharso, A.A. Adesina, D.L. Trimm, N.W. Cant, unpublished results.